

LA-UR-06-2946

Approved for public release;  
distribution is unlimited.

*Title:* RESIDUAL STRESS SOLUTION EXTRAPOLATION FOR  
THE SLITTING METHOD USING EQUILIBRIUM  
CONSTRAINTS

*Author(s):* Gary S. Schajer (Univ. of British Columbia)  
Michael B. Prime (ESA-WR)

*Submitted to:* Journal of Engineering Materials and Technology  
Vol 129, Number 2, pp. 226-232, 2007



Los Alamos National Laboratory, an affirmative action/equal opportunity employer, is operated by the University of California for the U.S. Department of Energy under contract W-7405-ENG-36. By acceptance of this article, the publisher recognizes that the U.S. Government retains a nonexclusive, royalty-free license to publish or reproduce the published form of this contribution, or to allow others to do so, for U.S. Government purposes. Los Alamos National Laboratory requests that the publisher identify this article as work performed under the auspices of the U.S. Department of Energy. Los Alamos National Laboratory strongly supports academic freedom and a researcher's right to publish; as an institution, however, the Laboratory does not endorse the viewpoint of a publication or guarantee its technical correctness.

# Residual Stress Solution Extrapolation for the Slitting Method using Equilibrium Constraints

Gary S. Schajer

Department of Mechanical Engineering,  
University of British Columbia, Vancouver, Canada

Michael B. Prime

Engineering Sciences and Applications Division,  
Los Alamos National Lab., Los Alamos, NM, USA

## **Abstract**

Established methods for calculating residual stresses from the strains measured when using the slitting method give results for the stresses that exist within the depth range of the slit. Practical considerations typically limit this range to about 90-95% of the specimen thickness. Force and moment equilibrium can provide additional information that may be used to estimate the residual stresses in the “no-data” region within the remaining ligament beyond the maximum slit depth. Three different numerical methods to calculate the residual stress profile over the entire specimen thickness are investigated. They are: truncated Legendre series, regularized Legendre series, and regularized unit pulses. In tests with simulated strain data and with strain data measured on a cold compressed 7050-T7452 Aluminum hand forging, the three methods gave generally similar stress results in the central region of the specimen. At small depths, where the strain sensitivity to the residual stresses is low, the two regularized calculation methods tended to give more stable results. In the area of very large depth beyond the maximum depth of the slit, the regularized Legendre series solution generally gave the most realistic stress results.

April, 2006

## Introduction

The Slitting Method [1, 2] is an effective technique for measuring residual stresses in beam and plate shaped materials. The method involves progressively relieving the local residual stresses by cutting a narrow slit from one side of the beam or plate, as schematically shown in Figure 1, in a series of small depth steps. The resulting strain reliefs are measured using a strain gage attached to the opposite surface.

Several technical challenges must be addressed to achieve reliable results. On the practical side, the strain and slit depth measurements must be made with great precision, and care must be taken not to induce extraneous residual stresses during the slit cutting process. The wire EDM process [3] has been shown to be an effective and accurate “low-stress” cutting process. Another practical challenge occurs when the cut has penetrated most of the material thickness, and the “free end” of the specimen is secured to the fixed part by only a thin remaining ligament of material. Under these conditions, it becomes difficult to support the weight of the free end without distorting the relieved strain readings. Doing the machining with the specimen oriented so that the advancing edge of the slit is vertical helps, but does not fully eliminate the problem.

On the theoretical side, it is a significant mathematical challenge to calculate the originally existing residual stresses from the measured strains. The relationship between the through-thickness residual stress distribution and the measured strains is an “inverse problem”. Such calculations are notoriously sensitive to the effects of measurement noise such that small strain data errors cause proportionally much larger stress solution errors. Typical solution methods involve expressing the stresses to be determined in the form of a mathematical series, and then solving for the series coefficients. The solution can be stabilized either by truncating the series at an intermediate number of terms, or by modifying the solution to penalize the effects of data noise.

A further characteristic of an inverse problem is that the spatial range of the solution corresponds to the spatial range of the data. Thus, for slitting, residual stresses can be calculated specifically for the part of the specimen thickness cut by the slit. The thickness of the specimen that remains uncut at the conclusion of the slitting measurements is excluded from the calculation. The desire to evaluate residual stresses over the greatest fraction of the specimen thickness encourages the wish to cut the slit as deeply as possible. However, the difficulty of

supporting the weight of the free end of the specimen, and the consequent strain data distortions, limits the maximum slit depth to about 0.90-0.95 of the total specimen thickness. An additional challenge that arises, specific to slitting, is that the finite length of the strain gage attached to the opposite surface influences the measured strain response, making it increasingly difficult to evaluate the corresponding theoretical strain responses accurately at very large slit depths.

In the case of slitting, force and moment equilibrium provide additional information to make an estimate of the “missing” stresses in the uncut ligament of the specimen. However, this calculation must be done with some care, otherwise the accumulated errors from the area within the slit depth will concentrate into the small uncut area, and will give greatly distorted results.

This paper describes three different methods for calculating residual stresses from slitting strain data. Equilibrium constraints are combined with these methods to get estimates of the stresses in the uncut ligament. Each method has its particular features, and can be the most desirable in some cases, and the least desirable in others. These characteristics are explored using both simulated and measured data. Recommendations are then made for a general-purpose stress calculation method.

## Residual Stress Calculations

The strain  $\varepsilon(a)$  measured when the slit has been advanced to a depth  $a$  depends on a combination of the stresses  $\sigma(x)$  at all depths  $x$  within the slit depth, as follows:

$$\varepsilon(a) = \frac{1}{E} \int_0^a c(a,x) \sigma(x) dx \quad (1)$$

The elastic constant  $E$  is the plane stress or plane strain Young’s modulus, chosen according to the thickness-to-width ratio of the specimen [4]. The kernel function  $c(a,x)$  describes the strain response due to a unit stress at depth  $x$  in a slit of depth  $a$ . This function depends on the geometry of the specimen and attached strain gage, and for slitting is typically evaluated numerically using finite element calculations [5].

Equation (1) is described as an “inverse problem” because the stresses  $\sigma(x)$  to be determined are within the integral, while the measured strain data  $\varepsilon(a)$  are outside. The

corresponding “forward problem” to calculate the strains from known stresses can be solved straightforwardly by direct integration. However, the inverse problem to find the stresses from the strains is more complex. An effective solution method is to represent the stress profile in the form of a mathematical series  $\phi_j(x)$  with coefficients  $A_j$  :

$$\sigma(x) = \sum_j A_j \phi_j(x) \quad (2)$$

The stress solution involves determining the initially unknown coefficients  $A_j$ . Substituting equation (2) into equation (1) gives:

$$\varepsilon(a) = \frac{1}{E} \sum_j A_j C_j(x) \quad (3)$$

where:

$$C_j(a) = \int_0^a c(a,x) \phi_j(x) dx \quad (4)$$

In theory, any form of series with linearly independent terms that spans the solution space (is able to represent any arbitrary stress profile), is acceptable. Two convenient choices are considered here, Legendre polynomials and unit pulse functions. Legendre polynomials have been frequently used for slitting calculations [2,6], where their particular advantage is that the terms of order 2 and higher automatically obey both force and moment equilibrium. An important consequence of this property is that the corresponding compliance functions  $C_j(a)$  are numerically well-conditioned and reach finite values as the slit approaches full depth.

Unit pulse functions are also a convenient choice because they have a simple interpretation and implementation [7]. Successive functions have a unit value within the successive steps in slit depth, and a zero value elsewhere. Thus, the coefficients  $A_j$  directly represent the stresses within each of the slit depth steps. The corresponding compliance functions  $C_j(a)$  can be expressed compactly in terms of the cumulative strain function. However, unit pulse functions do not automatically obey equilibrium, and therefore they do not remain finite as the slit approaches full depth. This singularity can be removed by weighting the compliance functions and strain data by the factor  $(t - a_j)^2$ , where  $t$  is the specimen thickness at

the slit. A convenient feature when using this weighting factor is that the corresponding compliance functions  $C_j(t)$  for the limiting case at  $a = t$  represent moment equilibrium [7].

For a strain measurement  $\varepsilon_i$  made at step  $i$  within a series of  $m$  slit depth steps  $a_i$ , equation (3) can be written in matrix format as:

$$\frac{1}{E} \mathbf{C} \mathbf{A} = \boldsymbol{\varepsilon} \quad (5)$$

where element  $C_{ij}$  of matrix  $\mathbf{C}$  is the value of compliance function  $C_j(a)$  evaluated at  $a = a_i$ . Solution of equation (5) gives the coefficients  $A_j$ , which can then be substituted in equation (2) to give the residual stress solution.

The noise sensitivity of inverse problem solutions causes small data errors to produce proportionally larger errors in the solution. For the slitting calculations described here, the poor numerical conditioning of matrix  $\mathbf{C}$  reflects this noise sensitivity. Two possible ways of improving the numerical conditioning in equation (5) are: use a limited number of series terms (truncation) [6], or use a noise penalization scheme such as Tikhonov regularization [7,8]. When using Legendre polynomials, either of these possibilities can be used. With unit pulse functions, regularization is practicable, but not series truncation.

When using a truncated Legendre series solution with terms of order 2 to  $n$  (lower orders are excluded because they violate equilibrium), matrix  $\mathbf{C}$  becomes an  $m \times n-1$  rectangular matrix. Equation (5) can be solved in a least-squares sense as:

$$\frac{1}{E} \mathbf{C}^T \mathbf{C} \mathbf{A} = \mathbf{C}^T \boldsymbol{\varepsilon} \quad (6)$$

Truncating the series at a low order  $n$  improves matrix conditioning and diminishes noise sensitivity (reduces data error). However, it also distorts the stress solution (increases model error) and reduces spatial resolution in the stress profile. An optimum choice of series truncation minimizes the sum of the data and model errors [6]. This procedure is used here.

Alternatively, Tikhonov regularization involves applying a penalty function on the stress solution to penalize and smooth out noise in the results. Common targets of the penalty function are the size, slope or curvature of the solution. Here, either the slope or the curvature is chosen as the target of the penalty function because noise tends to create many sharp peaks and dips in

the stress solutions, each corresponding to a large local slope or curvature. Inclusion of the penalty function modifies equation (5) to:

$$\frac{1}{E} \left( \mathbf{C}^T \mathbf{C} + \alpha \mathbf{D}^T \mathbf{D} \right) \mathbf{A} = \mathbf{C}^T \boldsymbol{\varepsilon} \quad (7)$$

Matrix  $\mathbf{D}$  is an operator that acts on the stress solution to identify its slope or curvature. For Legendre polynomials of order 2 to 6, matrix  $\mathbf{D}$  for slope penalization (“flat” regularization) and for curvature penalization (“smooth” regularization) are:

$$\mathbf{D}_{\text{flat}} = \begin{bmatrix} 6 & 0 & 6 & 0 & 6 \\ 0 & 12 & 0 & 12 & 0 \\ 6 & 0 & 20 & 0 & 20 \\ 0 & 12 & 0 & 30 & 0 \\ 6 & 0 & 20 & 0 & 42 \end{bmatrix} \quad \mathbf{D}_{\text{smooth}} = \begin{bmatrix} 18 & 0 & 60 & 0 & 126 \\ 0 & 150 & 0 & 420 & 0 \\ 60 & 0 & 690 & 0 & 1680 \\ 0 & 420 & 0 & 2310 & 0 \\ 126 & 0 & 1680 & 0 & 6300 \end{bmatrix} \quad (8)$$

In general, for Legendre polynomials of order 2 to  $n$ , the matrix elements for  $2 \leq j \leq i \leq n$  (the lower triangle) and  $i+j = \text{even}$  are:

$$(\mathbf{D}_{\text{flat}})_{ij} = j(j+1) \quad (\mathbf{D}_{\text{smooth}})_{ij} = \frac{(j-1)j(j+1)(j+2)}{24} [3i(i+1) - (j-2)(j+3)] \quad (9)$$

The odd-summed elements are zero. Since the matrices are symmetrical, the upper triangles can be completed by interchanging  $i$  and  $j$ . The matrices in equations (8) are computed by integrating the entire span of the Legendre polynomials, and thus, the regularization acts on the full width of the stress profile, not just the region of the slit depth.

When using unit pulse functions and equal slit depth steps, the matrices  $\mathbf{D}$  are:

$$\mathbf{D}_{\text{flat}} = \begin{bmatrix} 0 & & & & \\ -1 & 1 & & & \\ & -1 & 1 & & \\ & & -1 & 1 & \\ & & & -1 & 1 \end{bmatrix} \quad \mathbf{D}_{\text{smooth}} = \begin{bmatrix} 0 & 0 & & & \\ -1 & 2 & -1 & & \\ & -1 & 2 & -1 & \\ & & -1 & 2 & -1 \\ & & & 0 & 0 \end{bmatrix} \quad (10)$$

where the number of rows equals the number of slit depth steps used. Both matrices are banded around the main diagonal, with zeroes elsewhere. For flat regularization, all rows except the first

have  $[-1 \ 1 \ 0]$  centered along the main diagonal. For smooth regularization, all rows except the first and last have  $[-1 \ 2 \ -1]$  centered along the main diagonal.

The factor  $\alpha$  in equation (7) controls the amount of regularization that is applied. Excessively large regularization introduces so much smoothing that it distorts the underlying stress solution (model error). Conversely, insufficient regularization allows excessive noise (data error) to remain in the calculated stress results. Optimal regularization balances these two tendencies, minimizing distortion of the stress solution while removing most noise.

Optimal regularization can be identified by considering the misfit between the strains corresponding to the regularized stress solution and the measured strains:

$$\boldsymbol{\varepsilon}_{\text{misfit}} = \frac{1}{E} \mathbf{C} \mathbf{A} - \boldsymbol{\varepsilon} \quad (11)$$

The Morozov criterion [8] indicates that a misfit can be acceptable providing it is within the experimental error in the strain measurements. For the case where the standard errors of all the strain measurements are the same, the Morozov criterion is obeyed when the root mean square of the misfit equals to the standard error in the strain measurement. Thus:

$$\varepsilon_{\text{std}}^2 = \varepsilon_{\text{rms}}^2 = \frac{1}{m} \sum_{i=1}^m (\varepsilon_{\text{misfit}})_i^2 \quad (12)$$

For equally spaced slit depths steps, the standard error in the strain measurements may be estimated using [7] :

$$\varepsilon_{\text{std}}^2 = \sum_{i=1}^{m-3} \frac{(\varepsilon_i - 3\varepsilon_{i+1} + 3\varepsilon_{i+2} - \varepsilon_{i+3})^2}{20(m-3)} \quad (13)$$

The “optimal” value of the regularization factor  $\alpha$  in equation (7) that meets the Morozov criterion can be identified by iteration.

When using regularization with Legendre polynomials, the major part of the series representation is done by the lower-order terms. Beyond the 30<sup>th</sup> term, the coefficients typically drop below 1/1000 the size of the initial terms. Thus, to avoid having to calculate very high order Legendre compliance functions, the Legendre polynomials are limited to a maximum order 30 when using regularization. (By comparison, the truncation method typically limits the



maximum Legendre polynomial order within the range 6 to 12). A consequence of limiting the maximum Legendre polynomial order is that the polynomials don't quite fully span the stress solution space, and thus are not able to model the stress profile exactly. Thus, even with no regularization, there is a small strain misfit when evaluating equation (11).

Application of the Morozov criterion as a means of choosing optimal regularization works most effectively when zero regularization corresponds to zero strain misfit. This condition can be met by using the back calculated strains  $\boldsymbol{\epsilon}_{30} = (1/E) \mathbf{C} \mathbf{A}$  evaluated with all 30 Legendre polynomials and no regularization as the basis of the strain misfit calculation instead of the measured strains. In general, 30 is a sufficiently high order of polynomial that the difference  $\boldsymbol{\epsilon}_{30} - \boldsymbol{\epsilon}$  is small. An alternative, equivalent way of achieving the same objective is to continue to use the measured strains as the basis of the strain misfit calculation, augment the target standard error with the 30<sup>th</sup> order unregularized misfit:

$$\epsilon_{\text{target}} = \sqrt{\epsilon_{\text{std}}^2 + \epsilon_{30}^2} \quad (14)$$

and use  $\epsilon_{\text{target}}$  in place of  $\epsilon_{\text{std}}$  in equation (12). Both methods produce the same results.

## Tests with Simulated and Measured Data

A series of tests was undertaken to investigate the characteristics of various schemes for solving equation (1) to evaluate slitting residual stresses. Three main methods were investigated: Legendre series with truncation, Legendre series with regularization, and unit pulse series with regularization. Some minor variations of these methods were also investigated, for example, the use of "flat" or "smooth" regularization. The first tests were done using simulated strain data created using a "forward" solution of equation (1) using chosen stress profiles. Normally distributed random strain errors with a standard deviation of  $2\mu\epsilon$  were added to the strain data to simulate measurement noise. These tests were useful to evaluate the capabilities of the various solution methods to reproduce exactly known stress profiles. A final set of tests was done using measured strain data from practical slitting measurements with a quenched aluminum specimen.

Figure 2 shows the theoretical and the calculated residual stress profiles for a simulated beam type specimen made of a perfectly plastic material. A simulated bending load was applied

that loaded the material well into the plastic range, and then the load was released elastically. The thin dashed line in Figure 2 indicates the “theoretical” stress profile. The stress profile has a central elastic range of 20% of the total thickness, with stresses varying from 100MPa to -100MPa. This profile was chosen to investigate the capacity of the stress calculation methods to evaluate a practically occurring stress profile with sharply varying features. The associated strains were determined for the first 90% of the specimen depth, leaving the last 10% unspecified to correspond to the uncut material ligament. The vertical thin dashed line in Figure 2 indicates the maximum slit depth. No strain data are available corresponding to the region to the right of this line, so the stress evaluations there are extrapolations based on equilibrium and regularization.

In Figure 2 and subsequent graphs, the thin solid line indicates the residual stress profile calculated using regularized unit pulses, the thick solid line indicates the profile calculated using regularized Legendre polynomials, and the thick dashed line indicates the profile calculated using truncated Legendre polynomials. For this stress distribution, all three calculation methods produce similar results. They all show some rounding of the theoretically sharp boundaries between the inner elastic region and the outer plastically deformed regions. This rounding occurs because the stress calculation methods identify these sharp slope changes as “noise” and act to “smooth” them. Some differences in the stress curves are apparent at small depths, where strain sensitivity is very low, and in the “no-data” region within the remaining ligament beyond 0.9 normalized depth. Some oscillation is observed with the truncated Legendre series results. The regularized Legendre series and the regularized unit pulse calculations give more stable results that overlap for large depths.

In Figure 2 and subsequent graphs, the moment equilibrium that is automatically enforced when the pulse method is extrapolated to full slit depth [7] had to be modified. This change was necessary because the datum for the moment equilibrium was at the full-depth surface. Since the stress to be estimated in the uncut material ligament is immediately adjacent to that datum, the corresponding moment arm was very small, thereby producing stress evaluations that are prone to error. The datum for the moment equilibrium was shifted to zero specimen depth to avoid this behavior and to reduce the influence of the noise-sensitive surface stresses. This shift was made by subtracting  $2(a_i - a_{i-1})/t$  times the original row sum from the elements of the final row of matrix  $\mathbf{C}$  in equation (5). Even with this change, the equilibrium

stress result only gives the average stress in the whole of the uncut ligament. Thus, the best estimate of the stress profile in this area is a straight line passing through the mid-point. No further detail can be resolved.

Figure 3 shows a similar bending stress distribution to that shown in Figure 2, but with the central elastic region reduced to the range 0.45 to 0.55. The resulting sharp gradient changes at the elastic-plastic boundaries provide a more severe challenge to the stress calculation methods, resulting in the oscillations seen in the calculated stress profiles. Again, the truncated Legendre series solution shows the greatest oscillation, particularly at very small and very great depths. The regularized Legendre and regularized unit pulse methods give similar results, with the pulse method giving slightly better resolution of the central slope and gradient changes. Both the latter two calculations continue to give realistic stress estimations in the “no-data” region beyond 0.9 normalized depth.

The regularized calculations in Figures 2 and 3 used smooth (second derivative) regularization. Smooth regularization acts to try to straighten a curved stress profile. The regions most influenced by regularization are the small depth region because the strain sensitivity to stress is very low there, and the great depth region because there are no strain data available there. Thus, smooth regularization particularly tends to straighten the calculated stress profiles in these end regions. In the case of the bending stress profiles in Figures 2 and 3, the stress profile was actually straight in these regions, so there was no adverse consequence. However, if there were significant curvatures in these regions, some local distortion could occur. To investigate this point, an additional simulated stress profile in the form of a cosine curve was chosen. This stress profile has maximum curvature at the ends. Again the calculated strain response from the forward solution of equation (1) was augmented with normally distributed random errors with standard deviation of  $2\mu\epsilon$  to simulate measurement noise.

Figure 4 shows the calculated stress profiles for the simulated cosine curve data. As before, the results from all calculation methods are similar. For this smoothly varying stress profile, the truncated Legendre series solution gives the closest result. As expected, both regularized solutions tend to over-straighten the calculated stress profile at small depths, and to a lesser extent at great depths. The regularized unit pulse solution shows some minor oscillations. These are caused by the standard strain error estimate from equation (13) evaluating slightly low,

1.8 $\mu\epsilon$  instead of 2 $\mu\epsilon$ . (The strain error estimates for Figures 2 and 3 were accurate within 0.05 $\mu\epsilon$ ). Thus, the amount of regularization used for Figure 4 is somewhat less than ideal. Increasing the target misfit to 2 $\mu\epsilon$  almost entirely removes the oscillations. This experience suggests that it may be desirable occasionally to increase the target misfit by 10-15% over the estimated standard strain error to damp out any undesirable oscillations that may occur.

Figure 5 shows the stress profiles for the simulated cosine curve data, calculated using flat regularization. Flat regularization tends to reduce the local gradient of the stress profile, particularly at the ends. Here, both Legendre polynomial methods give flatter gradients at both small and great depths, which in this example is a more realistic behavior. However, the difference between flat and smooth regularization is modest overall.

Slitting strain measurements were done on a 107.2mm thick heat-treated and quenched 7050-T7452 aluminum billet hand forging, similar to forgings measured with other techniques [9,10]. The forging was solution heat-treated, subject to a 70 °C quenchant of water with dissolved gas [11], and then partially stress relieved by multiple cold compressions. A slit was cut in the billet to a normalized depth of 0.94 in 60 depth increments using wire EDM machining. Figure 6 shows the stresses calculated by the various methods from the measured strain data. In this case, the actual residual stress profile is not independently known, so no absolute comparisons of the stress result are possible. However, it is expected from the specimen preparation that the residual stress profile should be generally symmetrical. The calculated stress profiles in Figure 6 follow the same pattern observed with the simulated data. The results from the regularized Legendre series and unit pulses are almost identical within the slit depth, but differ in the “no-data” region to the right of the vertical dashed line. In this case, the straight-line approximation available from the unit pulse method is not adequate to represent this curved part of the stress profile. The regularized Legendre series method gives more realistic-looking results, in particular showing a satisfying left-to-right symmetry. The truncated Legendre series method gives broadly similar results, smoother in the central area, and with slightly displaced stress peak at low depths. Without any independent comparison, it is not possible to assess the absolute quality of the various stress solutions. Perhaps the small oscillation at the center is an artifact, but its almost identical reproduction by both regularized Legendre and unit pulse methods suggests that it may be a real detail.

## Conclusions

The three slitting residual stress calculations investigated here: truncated Legendre series, regularized Legendre series, and regularized unit pulses, were found to give generally similar calculated stress results, particularly in the central depth region, away from the boundary areas where the depth is either very small or very large. The area of very large depth encompasses the region beyond the maximum depth of the slit, within which no strain data are available. The stresses in this region are estimated using equilibrium, based in the strain measurements within the range of the slit depth. In general, the regularized Legendre series solution gives the most consistent stress results for the region of the remaining material ligament.

The strain sensitivity to residual stresses is low at small slit depths, and consequently stress evaluations in this area have more uncertainty than elsewhere. The truncated Legendre series method often reflects this uncertainty with localized oscillations. The regularized Legendre and unit pulse methods generally give more stable results. However, regularization type can influence the stress solution in this region, with smooth regularization generating straight-line profiles, and flat regularization generating horizontally turning curves. These effects are localized, and in general both regularization type give satisfactory results. “Flat” regularization is numerically simpler, while “smooth” regularization is sometimes more stable.

Each of the three stress calculation methods discussed here is effective, and each has its own particular features. The truncated Legendre series method can sometimes smooth out potential artifacts in the calculated stress profile. The unit pulse method is conceptually straightforward and has the best capability to resolve steep stress gradients and sharp curves within the range of the slit depth. It can also give reasonable estimates of the stresses within the uncut region beyond the slit depth, but not always with a realistic shape. The regularized Legendre method has almost the same capability to resolve steep stress gradients and sharp curves within the range of the slit depth. In addition, it also has a good capability to give realistic estimates of the stresses within the uncut region beyond the slit depth. For this reason, the regularized Legendre series method is suggested as a general-purpose residual stress calculation method to be used when an estimate of the stresses within the uncut region is desired. Either smooth or flat regularization can be used, depending on the expected shape at the edges of the stress profile.

## Acknowledgments

This work was financially supported by the Los Alamos National Laboratory, NM, USA, operated by the University of California for the United States Department of Energy under contract W-7405-ENG-36, and by the Natural Sciences and Engineering Research Council of Canada (NSERC).

## References

1. Cheng, W., and Finnie, I., 1986, "Measurement of Residual Hoop Stress in Cylinders Using the Compliance Method," *Journal of Engineering Materials and Technology*, **108**, pp.87-92.
2. Prime, M. B., 1999, "Residual Stress Measurement by Successive Extension of a Slot: The Crack Compliance Method," *Applied Mechanics Reviews*, **52**(2), pp.75-96.
3. Cheng, W., Finnie, I., Gremaud, M., and Prime, M. B., 1994, "Measurement of near-Surface Residual-Stresses Using Electric-Discharge Wire Machining," *Journal of Engineering Materials and Technology-Transactions of the ASME*, **116**(1), pp. 1-7. .
4. Schindler, H. J., Cheng, W., and Finnie, I., 1997, "Experimental Determination of Stress Intensity Factors due to Residual Stresses," *Experimental Mechanics*, **37**(3), pp. 272-277.
5. Rankin, J. E., and Hill, M. R., 2003, "Measurement of Thickness-Average Residual Stress near the Edge of a Thin Laser Peened Strip," *Journal of Engineering Materials and Technology*, **125**(3), pp. 283-293.
6. Prime, M. B., and Hill, M. R. 2006. "Uncertainty, Model Error, and Order Selection for Series-Expanded, Residual-Stress Inverse Solutions." *Journal of Engineering Materials and Technology*, **128**(2), pp.175-185.
7. Schajer, G. S., and Prime, M. B. 2006. "Use of Inverse Solutions for Residual Stress Measurements". *Journal of Engineering Materials and Technology*. To appear.

8. Tikhonov, A., Goncharsky, A., Stepanov, V., and Yagola, A., 1995, "Numerical Methods for the Solution of Ill-Posed Problems," Kluwer, Dordrecht.
9. Prime, M. B., Newborn, M. A., and Balog, J. A., 2003, "Quenching and Cold-Work Residual Stresses in Aluminum Hand Forgings: Contour Method Measurement and FEM Prediction," *Materials Science Forum*, **426-432**, pp. 435-440.
10. Tanner, D. A., and Robinson, J. S., 2003, "Modelling Stress Reduction Techniques of Cold Compression and Stretching in Wrought Aluminium Alloy Products," *Finite Elements in Analysis and Design*, **39**(5/6), pp. 369-386.
11. Yu, H, Nicol, J. A., Ramser, R. A., Hunter, D. E., 1997, "Method of heat treating metal with liquid coolant containing dissolved gas," U. S. Patent 5,681,407.

## List of Figures

- Figure 1. Schematic diagram of the slitting method.
- Figure 2. Calculated residual stresses for a simulated bending specimen with central elastic region between 0.40 and 0.60 normalized depth. The regularized solutions use “smooth” regularization, and the truncated Legendre series contains terms up to 12<sup>th</sup> order.
- Figure 3. Calculated residual stresses for a simulated bending specimen with central elastic region between 0.45 and 0.55 normalized depth. The regularized solutions use “smooth” regularization, and the truncated Legendre series contains terms up to 11<sup>th</sup> order.
- Figure 4. Calculated residual stresses for a simulated quenched specimen. The regularized solutions use “smooth” regularization, and the truncated Legendre series contains terms up to 7<sup>th</sup> order.
- Figure 5. Calculated residual stresses for a simulated quenched specimen. The regularized solutions use “flat” regularization, and the truncated Legendre series contains terms up to 7<sup>th</sup> order.
- Figure 6. Calculated residual stresses for a quenched aluminum specimen. The regularized solutions use “smooth” regularization, and the truncated Legendre series contains terms up to 11<sup>th</sup> order.



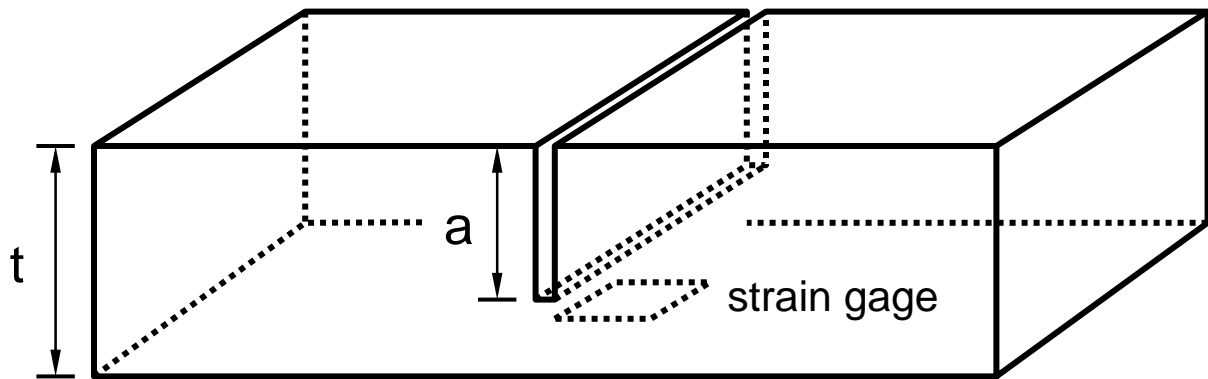


Figure 1. Schematic diagram of the slitting method.

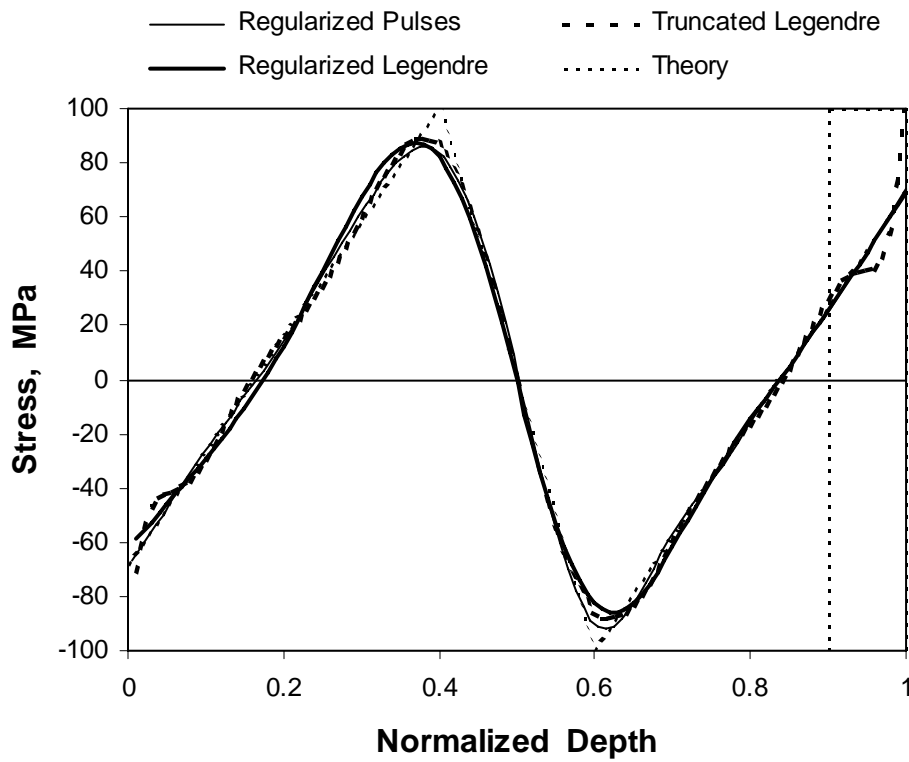


Figure 2. Calculated residual stresses for a simulated bending specimen with central elastic region between 0.40 and 0.60 normalized depth.

The regularized solutions use “smooth” regularization, and the truncated Legendre series contains terms up to 12<sup>th</sup> order.

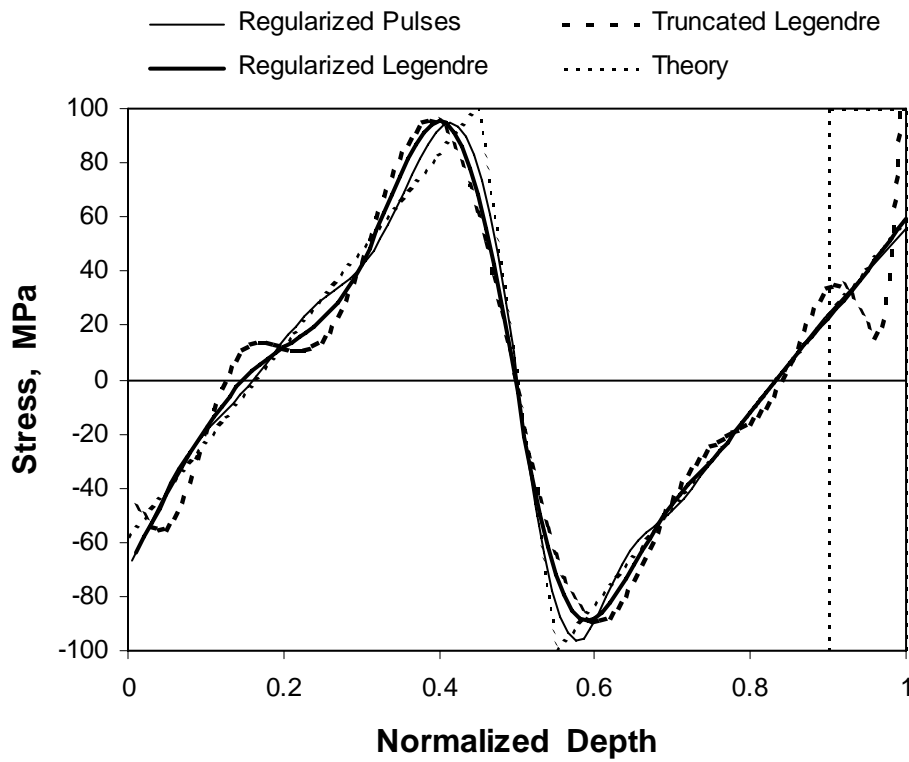


Figure 3. Calculated residual stresses for a simulated bending specimen with central elastic region between 0.45 and 0.55 normalized depth.

The regularized solutions use “smooth” regularization, and the truncated Legendre series contains terms up to 11<sup>th</sup> order.

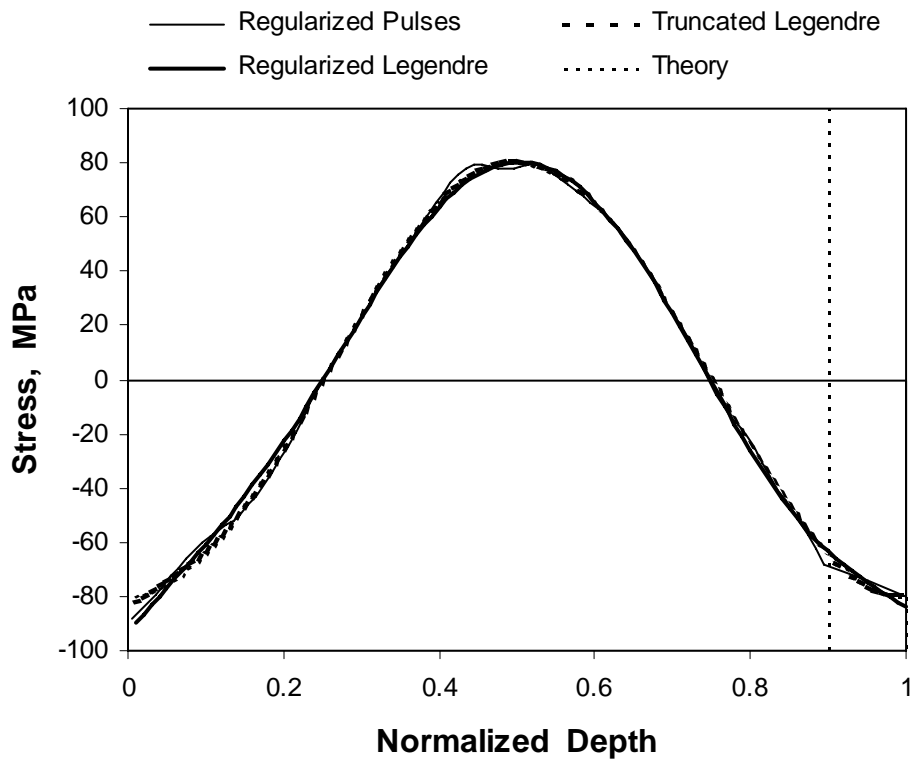


Figure 4. Calculated residual stresses for a simulated quenched specimen.

The regularized solutions use “smooth” regularization, and the truncated Legendre series contains terms up to 7<sup>th</sup> order.

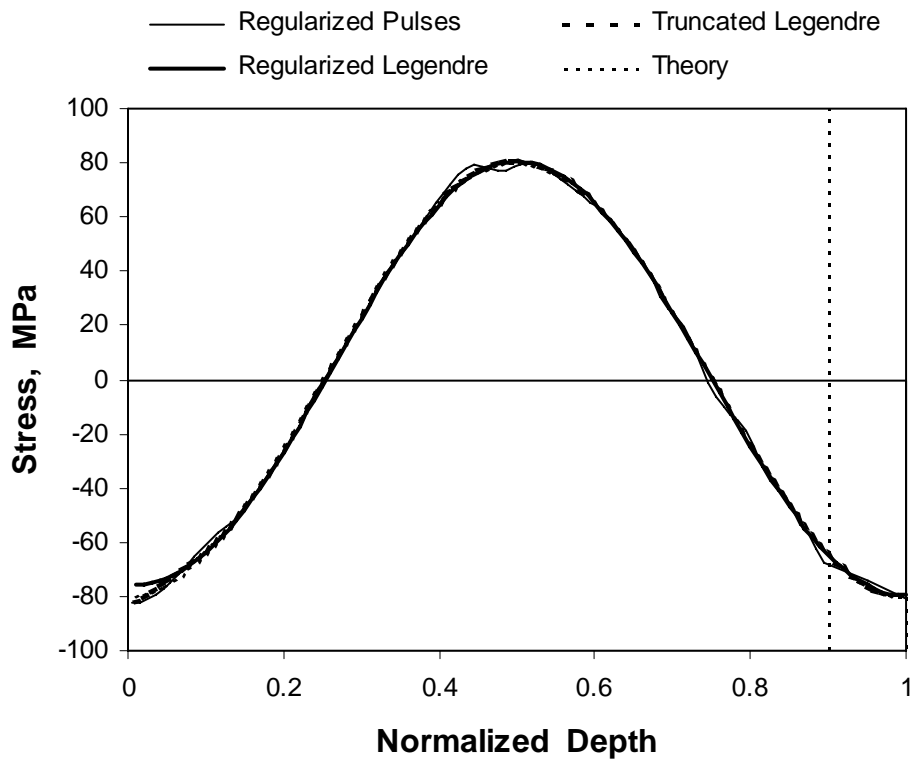


Figure 5. Calculated residual stresses for a simulated quenched specimen.

The regularized solutions use “flat” regularization, and the truncated Legendre series contains terms up to 7<sup>th</sup> order.

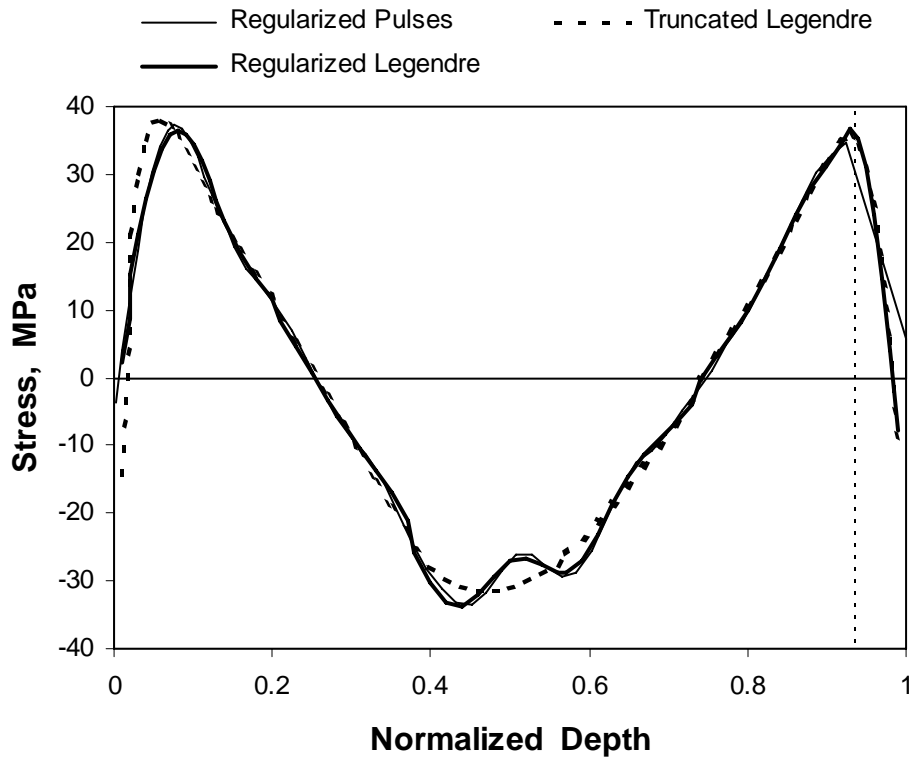


Figure 6. Calculated residual stresses for a quenched aluminum specimen.

The regularized solutions use “smooth” regularization, and the truncated Legendre series contains terms up to 11<sup>th</sup> order.